Characterization of cellulose microfibril foams in contact with plasma discharges in an AP-DBD experimental setup

L-F. Meunier[1,2], J. Profili[2], N. Naudé[1], and L. Stafford[2]

[1]*LAPLACE, Université de Toulouse, CNRS, INPT, Université Toulouse III – Paul Sabatier (UPS), Toulouse, France*
[2]*Département de Physique, Groupe PPHARE, Université de Montréal, Québec, Canada*

Abstract: Atmospheric Pressure Dielectric Barrier Discharge (AP-DBD) were characterized in helium gas in the presence of a microporous cellulose microfibril foams. It was found that higher frequency discharges had an electrical signal resembling a traditional glow discharge, but CCD images showed the presence of microdischarges. It was also found that higher frequency excitation of the sinusoidal applied voltage generated more surface damage to the foam than at lower frequency.

Keywords: Cellulose microfibril foams, AP-DBD, plasma-cellulose interactions.

1. Introduction

Over the past few years, the demand for renewable products issued from bio-based materials have increased constantly. This has brought forth an intense use of cellulose-based products as well as an increase in research related to their technological valorisation. For instance, crystalline nanocellulose has been applied to composite biomaterials to increase its mechanical strength. Nano cellulose and microfibrils have also been used to selectively filter heavy metals from certain liquids and are actively considered as an alternative material for food packaging applications [1,2,3,4,5].

These promising results have encouraged the developments of numerous cellulose-based products. Recently, the synthesis of highly controlled cellulosic foams with micro and nanoscale porosity has been proposed in the literature [1,2,4]. These substrates have revealed interesting morphological properties such as a small volumetric density, a weak thermal conductivity, and a very high surface area [1,4]. In this context, these characteristic features possess a great potential for the development of biodegradable selective chemical filters [5] or bio-based thermal barrier materials [1,2]. However, their commercialisation remains very limited due to their high hydrophilicity and hygroscopicity (high sensibility of a substrate to water and humidity).

Many aspects of the plasma's behaviour, when breakdown occurs with the foam in its epicentre, is poorly understood. This work is focused on how non-thermal plasmas at atmospheric pressure can be used to improve and/or change the foam's properties. The main goal in this work is to study the different discharge regimes that can be obtained when the plasma is sustained in the presence of the cellulose microfibril foams occupying the gas gap.

2. Experimental setup

The experiments were conducted using a closed chamber within which a plane-plane DBD cell was placed. The latter comprised of two silver electrodes deposited on alumina plates. Each electrode is square shaped, 3.8 cm in length. The gaseous gap between the dielectrics was set using two glass slides to the sides. A schematic of the experimental setup can be found on figure 1:

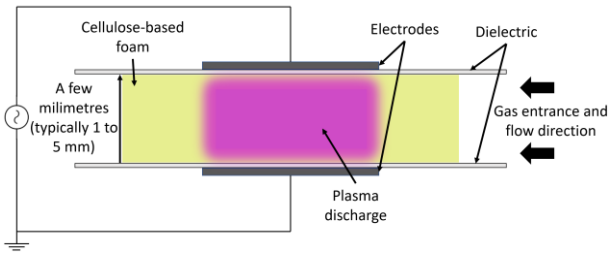

Fig 1. Experimental schematic of the cell discharge

The cellulose microfibril foam, hereby referred to as foam, were produced by a Canadian industrial partner named FPInnovations®. The cellulosic substrates were then shipped to our laboratory where they were cut in 4 cm by 7 cm rectangles and delicately placed between both electrodes in a plane-to-plane dielectric barrier discharge at atmospheric pressure. The size of the foams was slightly greater than that of the electrodes to insure a good contact with all the dielectric cell components and avoid any parasitic breakdown. Kapton tape was used to properly secure the foam at both extremities onto the dielectric.

The electrical signal was produced by using a waveform generator (Française d'Instrumentation model FI 5104). The frequencies were varied between 10 kHz and 60 kHz. The signal was amplified by a power amplifier (Crest Audio CA18 Professional Power Amplifier) and visualised on an oscilloscope (Teledyne Lecroy Wavesurfer 3024 Oscilloscope). All discharges were characterized by comparing the results obtained from the oscilloscope and the optical images were taken using a high-speed camera (QImaging QIClick 74-0083-A0 camera). Multiple pictures were taken on both the positive and negative current alternance of the plasma discharge. The exposure time was set to ten microseconds, and the gain was set to maintain appropriate lighting. Every image presented will be in identical conditions. All substrate surfaces were also observed before and after plasma treatment with an optical microscope (Keyence optical microscope model VHX-1000E).

Prior to each experiment, the chamber was purged under vacuum for thirty minutes to remove as many excess parasitic gaseous species as possible. Then, ten L/min of helium gas was introduced into the chamber.

3. Results

Figure 2 shows the current-voltage characteristics obtained in a pure helium discharge, and a helium discharge with important amounts of impurities from ambient air, both without foam, as a reference frame. In order to examine the role of impurities, helium gas was added to the inter-electrode gap and a plasma was immediately lit without pumping the residual gases following the closing of the chamber. Maintaining identical conditions as those found in both setups, it is possible to compare the effects of said impurities (labelled as "clean" and "parasitic"). On figure 2, a sinusoidal potential signal is sent at a peak-to-peak value of 3 kV. The two black curves are for the helium discharge in the presence of parasitic ambient air and the red ones are in the absence of said parasites. The sinusoidal signals correspond to the voltage axis while the others to the current axis.

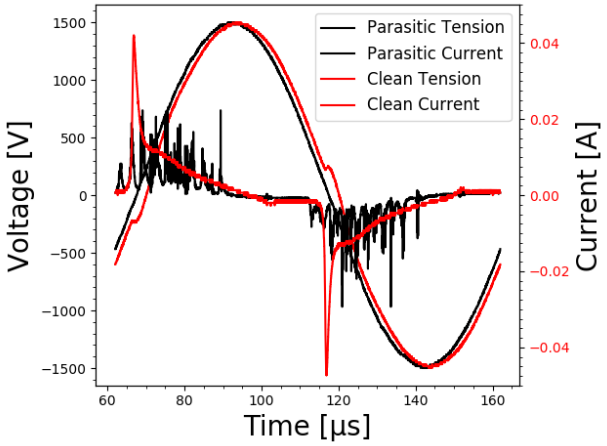

Fig. 2. Current-voltage characteristics of a pure and impure Helium discharge at 3 kVpp, 10 kHz, 2 mm gas gap, 10 slm He

Despite the voltage curve not changing dramatically from one condition to the other, the current curve does not act the same. The curve corresponding to the pure helium discharge is often depicted as a glow discharge with a single peak per half-cycle of the applied voltage [6,7]. On the other hand, the curve corresponding to the impure helium discharge resembles what is typically referred to as a filamentary discharge [6,7].

It is, however, wrong to assume the nature of the discharge solely on electrical measurements [6]. It is necessary to also take optical measurements using a camera [6,7]. *Figures 3* through *6* are pictures taken of the discharge over a single period. Gas entry is on the right side of the image and exit on the left. Light is more intense on the right side of the images. In the presence of impurities, Massines *et al*. have proposed that plasma will light more easily where the amount of impurities proportional to the amount of helium gas is smallest [6]. This increase in luminosity could be attributed to the smaller concentration of these impurities as opposed to the amount of helium gas at that point in space. For the sake of brevity, only one picture of both current alternances will be presented.

Fig. 3 and 4. Positive (top) and negative (bottom) current alternance of the clean discharge at 3 kVpp, 10 kHz, 2 mm gas gap, 10 slm He.

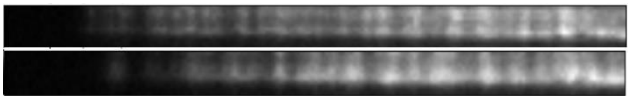

Fig. 5 and 6. Positive (top) and negative (bottom) current alternance of the parasitic discharge 3 kVpp, 10 kHz, 2 mm gas gap, 10 slm He.

Note that the top images of the pairs have the anode at the top, and the bottom images the anode at the bottom [6,7]. *Figures 3* and *4* show the discharge variation from one alternance to the other [7]. This is typical of glow discharges [6,7]. *Figures 5* and *6* do not demonstrate these alternances. Instead, a pattern of brighter and darker light can be observed. This is typical of a filamentary discharge and indicate prioritised microdischarges from one electrode to the other [6,7].

The presence of foam had a very strong effect on the physics of the discharge. The regime was destabilised and tended more easily towards a filamentary discharge. The addition of the foam was similar to the addition of impurities in the discharge shown demonstrated in *figure 2*.

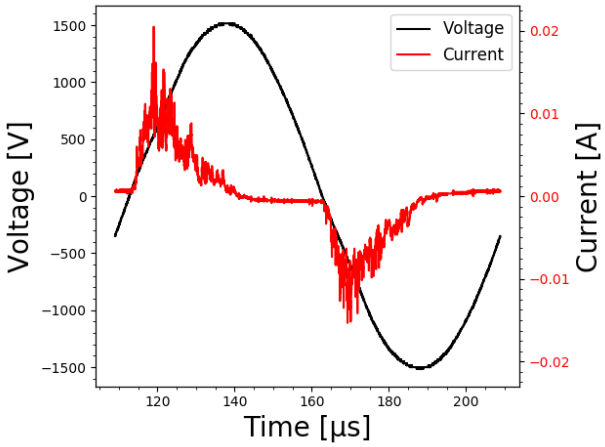

Fig. 7. Current-voltage characteristics of a Helium discharge in the presence of a foam at 3 kVpp, 10 kHz, 2 mm gas gap, 10 slm He

Additional measurements were taken in order to better understand how the plasma reacts within as well as around the foam, and what conditions made the discharge tend towards a seemingly more homogeneous distribution. *Figures 7* and *8* show two discharges in the presence of a microfibril cellulose foam. *Figure 7* was taken in pure

helium gas and a sinusoidal potential signal with a peak-to-peak value of 3 kV was sent. 10 SLM, 2 mm inter-electrode gap, and a frequency of 10 kHz were used. *Figure 8* was taken in the same conditions, save for frequency which was increased to 60 kHz.

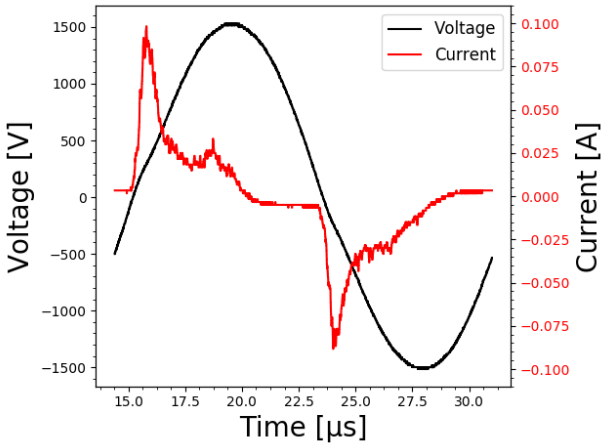

Fig. 8. Current-voltage characteristics of a Helium discharge in the presence of a foam at 3 kVpp, 60 kHz, 2 mm gas gap, 10 slm He

The increase in frequency from *figure 7* and *figure 8* increased the current detected in the discharge. An increase in frequency generates an increase in power [6,7], transferring directly to an increase in current. Whereas *figure 7* gives a filamentary-like electrical current, increasing the frequency to a value of 60 kHz changes the measurements to ones resembling more like a glow discharge [6,7]. A comparison can be directly made with *figure 2*. It is important to pursue this analysis further. To do so, photos using the camera were taken.

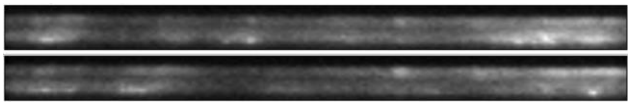

Fig. 9. Positive (top) and negative (bottom) current alternance of a pure helium discharge in the presence of foam at 3 kVpp, 10 kHz, 2 mm gas gap and 10 slm He

Fig. 10. Positive (top) and negative (bottom) current alternance of a pure helium discharge in the presence of foam at 3 kVpp, 60 kHz, 2 mm gas gap and 10 slm He

The top images of the pairs have the anode at the top, and the bottom images the anode at the bottom [6,7]. The bright spots that can be seen randomly distributed over the image seem to indicate filamentary discharge canals that have frayed their way through the foam. Otherwise, a relatively constant background light can be observed throughout the foam.

In order to better visualise the effect of the plasma discharge on the foams, an optical microscope was used to analyse in greater detail its surface. To do so, multiple images were stitched together, enhanced one hundred times, to see how the surface of the foam was damaged in relation to the plasma discharge in its presence. *Figure 11* shows a zoomed in portion of the foam used in the discharge found in *figures 7* and *9*:

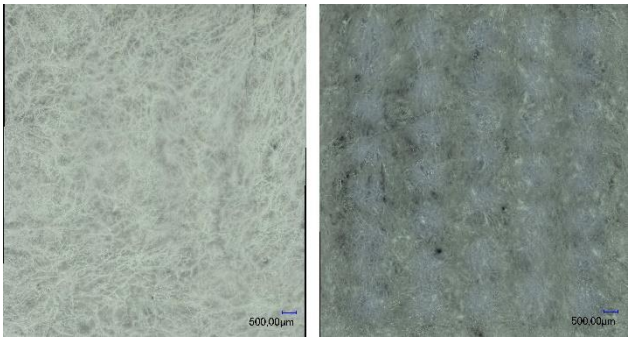

Fig. 11. Optical microscope image of the foam used in figures 7 and 9. The right image corresponds to the side of the foam closest to gas entry point and the left image to the gas exit point.

Another set of images were stitched together of the foam characterized in *figures 8* and *10*:

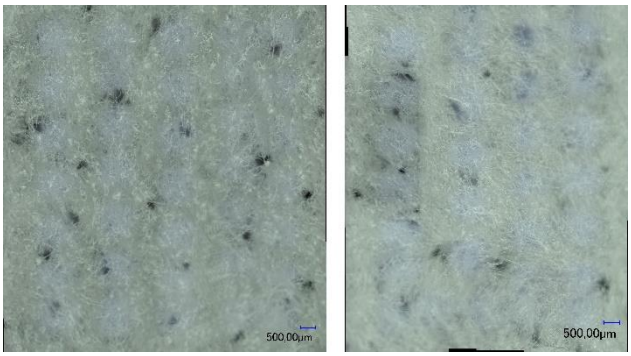

Fig. 12. Optical microscope image of the foam used in figures 8 and 10. The right image corresponds to the sides of the foam closest to gas entry point and the left image to the gas exit point.

As can be seen by comparing *figures 11* and *12*, a lot more damage can be found on the foam subject to a 60 kHz plasma. This can be attributed to the fact that power is higher in a plasma with higher frequency, keeping all other variables the same [6,7]. Furthermore, a closer analysis of the pictures taken on the surface of the foam subject to the 10 kHz plasma seems to indicate that more damage was done to the section of the foam closest to the gas flow entry. This behavior does not seem to exist on the foam on *figure 12*. There, it seems to be possible to find holes randomly distributed over the surface without any specific pattern.

To further understand the hole formation process and their approximate dimensions on the surface of the foam, depth composition images were taken at a five hundred times zoom.

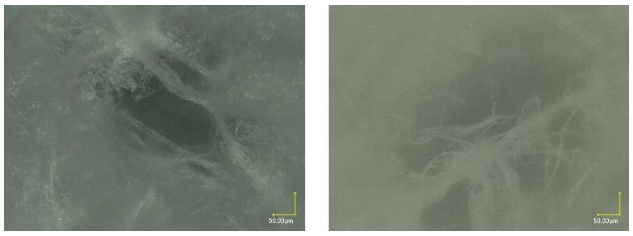

Fig. 13. Depth composition image of a hole on figure 11 (right) and 12 (left) at same zoom and scale.

Holes are therefore much more clearly defined on the foam treated at 60 kHz. This is due to the intensified current that can be measured on *figure 8*. These holes change the physical properties of the foam which in turn affects the plasma discharge behavior in the foam [1,2].

4. Conclusion

Plasma processes and behaviours were analysed to further the understanding of how plasmas coexist with a cellulose microfibril foam in an atmospheric pressure dielectric barrier discharge. For the purpose of this abstract, attention was dedicated to the behaviour of helium gas within the confines of this physical setup. It was shown that appropriate purity of the reactor is of vital importance in assuring a seemingly more homogeneous discharge. Moreover, certain conditions were analysed into which setup prioritised a discharge behaviour that favoured the latter as opposed to a filamentary one.

To better understand the damages incurred by the foam following treatment by plasma discharge, optical microscopy analyses were done, and the holes generated on the foam surface by the filaments were also analysed. It was found that a higher frequency discharge in the presence of a foam generated electrical results that seemed to tend towards a glow discharge, however generated significantly more damage to the foam.

These results are extremely promising in promoting the use of these cheap, environmentally friendly, porous foams in the industrial markets of today. A more in-depth analysis will be made on many different fronts to ensure a rigorous scientific process and to also ensure that every possible aspect of a plasma discharge is understood when done within this foam. This includes nominally pure helium plasma conditions but also helium plasmas in presence of reactive species, for example oxygen and hexamethyldisiloxane for plasma-enhanced chemical vapor deposition of functional coatings.

5. References

[1] I. Siró *et al*, Springer Sc.+Bus. Media, **17**, 3 (2010)

[2] C. Miao *et al*, Springer Sc.+Bus. Media, **20**, 5 (2013)

[3] S.M. Mukhopadhyay *et al*, Appl. Surf. Sc., 225 (2004)

[4] R.P. Edwin *et al*, Carbohydrate Polymers, **93**, 1 (2013)

[5] V. Armenise *et al*, IEEE NMD Conference (2016)

[6] F. Massines *et al*, European Physical J.Appl. Phys, **47**, 2805 (2009)

[7] F. Massines *et al*, Plasma Phys. Control. Fusion, **47**, 12B (2005)